



Review

Agostic interactions in alkyl derivatives of sterically hindered tris(pyrazolyl)borate complexes of niobium

Michel Etienne^a, John E. McGrady^b, Feliu Maseras^{c,d,*}^a Laboratoire de Chimie de Coordination du CNRS, UPR 8241, liée par conventions à l'Université Paul Sabatier et à l'Institut National Polytechnique de Toulouse, 205 Route de Narbonne 31077, Toulouse Cedex 04, France^b WestCHEM, Department of Chemistry, Joseph Black Building, University of Glasgow, G12 8QQ, UK^c Institute of Chemical Research of Catalonia (ICIQ), Avda. Països Catalans 16, 43007, Tarragona, Catalonia, Spain^d Departament de Química, Universitat Autònoma de Barcelona, 08193 Bellaterra, Catalonia, Spain

Contents

1. Introduction	635
2. Experimental data	637
2.1. Primary alkyl complexes	637
2.2. Acyclic secondary alkyl complexes	639
2.3. Cyclic (secondary) alkyl complexes	640
2.4. Cyclopropyl complexes: a rare example of an α -CC agostic interaction	641
3. Hybrid DFT/MM studies	641
4. The electronic origin of agostic interactions	643
5. Concluding remarks	645
Acknowledgements	645
References	645

ARTICLE INFO

Article history:

Received 4 April 2008

Accepted 29 July 2008

Available online 7 August 2008

Keywords:

Agostic interactions

Niobium complexes

Density functional theory

Density functional theory/molecular mechanics

ABSTRACT

This review describes how the joint experimental and computational study of a series of niobium(tris(pyrazolyl))(chloride)(alkyne)(alkyl) complexes has unearthed a very rich chemistry involving a variety of agostic interactions between the alkyl chain and the niobium centre. α and β C–H agostic, as well as α C–C agostic coordination, have been observed, in some cases in dynamic equilibrium within the same complex. The application of experimental and computational (DFT and DFT/MM) techniques reveals the subtle interplay of steric and electronic interactions that control the relative stability of these species. This analysis also sheds light on the electronic origin of agostic distortions in early transition metal centres.

© 2008 Elsevier B.V. All rights reserved.

1. Introduction

The precise nature of the interaction between a C–H group and a metal atom has been the centre of lively debate ever since the term ‘agostic bonding’ was coined by Green in 1983 [1,2]. An ‘agostic interaction’ is one where a C–H bond on an appended hydrocarbon ligand is brought into close proximity to the metal centre through a distortion of the ligand. The C–H bond in question can, in principle, be sited on an α -, β -, γ -, δ - or even more remote carbon centre, but

the discussion in this review will be restricted to the α - and β -CH cases shown in Chart 1.

The position of the hydrogens is obviously the most direct evidence for the presence of an agostic interaction, but the location of these light atoms by X-ray crystallography is problematic. X-ray crystallography measures the electron density, and the positions of nuclei are deduced from the electron density plot, the underlying assumption being that the maxima in electron density are defined by the core electrons, which in turn are coincident with the nucleus. This argument is not, however, valid when dealing with an atom with no core electrons (hydrogen), especially when it lies close to transition metal atoms with high electron densities. As a result, attention has been focussed largely on the structure of the

* Corresponding author at: Institute of Chemical Research of Catalonia (ICIQ), Avda. Països Catalans, 16, 43007 Tarragona, Spain.

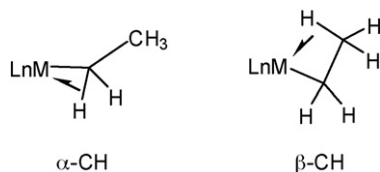


Chart 1. α - and β -CH agostic alkyls.

alkyl backbone: a β -CH agostic structure is best characterized in the solid state by a distortion of the alkyl group such that the angle $M-C\alpha-C\beta$ is significantly less than the standard value of 109.5° for an sp^3 hybridised $C\alpha$ carbon. The $C\alpha-C\beta$ bond is also typically somewhat shorter than those in a saturated hydrocarbon, indicating some double character, particularly for late transition metal complexes. All these features are consistent with the view that the agostic interaction maps out the early stages of β -hydride transfer, which would lead ultimately to a metal olefin hydride structure. The β -CH agostic distortion naturally requires some rearrangement of the metal coordination sphere to accommodate the presence of an additional ligand (the β -CH bond), and in cases where the coordination sphere is already crowded, α -CH structures may be adopted instead (Chart 1). This class of agostic complexes is particularly common for early transition metals in the absence of β -CH hydrogens. In contrast to their β -agostic counterparts, the characteristic geometric feature of an α -agostic complex is an opening of the $M-C\alpha-C\beta$ angle, sometimes to very obtuse values and a shortening of the $M-C\alpha$ bond.

Given the problems associated with locating the hydrogen atoms, the most reliable method to assign an agostic structure, at least for soluble complexes, is its NMR spectrum, although analysis is often complicated by dynamic processes. Whatever the position of the metal in the transition series or the type of agostic distortion (α - or β -CH), a lowering of the coupling constant $^1J_{CH}$ corresponding to one of the $^{13}C-^1H$ bonds is observed. The lowering is most important for β -CH structures: values from 110 Hz (α -CH) down to 35 Hz (β -CH) can be observed, compared to an average value of 120–130 Hz for a saturated alkyl group. β -agostic protons and carbons are usually also shielded in late transition metal complexes (although much less dramatically in early transition metal complexes) while α -agostic carbons are usually deshielded in early transition metal complexes.

The donation of the electrons in the $C-H$ σ bond to the metal centre [3] in a 3-centre-2-electron model [4] is the textbook explanation for this phenomenon, although the resemblance to η^2 -coordinated diatomic ligands such as H_2 has encouraged speculation that back-donation into the $C-H$ σ^* orbital may play a role [5,6]. The abundance of agostic complexes of transition metals with a formal d electron count of zero does however suggest that back-donation cannot be the dominant mechanism in all cases. The earliest theoretical studies of agostic bonding using Extended Hückel theory suggested that overlap between metal and $C-H$ σ orbitals was indeed significant in β -CH agostic complexes, offering support for the 3-centre-2-electron model [7]. In contrast, sharing of electron density between the hydrogen and the metal appears to be negligible in the α -agostic analogues, and Eisenstein instead proposed that the short $M \cdots H$ separation was caused by a canting of the alkyl group in order to optimise the strength of the $M-C$ bond [8,9]. Over the past decade, qualitative theoretical models such as Extended Hückel theory have largely been replaced by density functional theory (DFT), which offers chemically accurate total energies. Perhaps most significantly, the facility to optimise structural parameters with a high degree of accuracy has allowed hydrogen atoms to be located with some confidence – so-called

computational crystallography [10]. In parallel, the development of analysis tools such as quantum theory of atoms in molecules (QTAIM) [11] has encouraged several groups to re-assess the nature of the agostic bond. Within the QTAIM model, the presence of a bond critical point (BCP) is defined as a point between two nuclei where the gradient of the electron density vanishes [11d]. It has been proposed that the existence of such a BCP is a necessary and sufficient condition for the existence of a chemical bond between the two atoms concerned, although this definition has been questioned by a number of authors who have located such critical points between atoms which clearly do not share a chemical bond, at least in the sense commonly understood by chemists [12]. In the context of agostic complexes, Popelier has described the topology of the electron density in the archetypal β -agostic bond in $[(C_2H_5)_2TiCl_2]^+$, and argued that the presence of a BCP between the metal and the β hydrogen is indicative of a β -C–H agostic bond [13]. It is not clear, however, whether this argument can be generalised, because Scherer and co-workers have shown, for a series of d^0 metal alkyls, that the appearance of a BCP between metal and the β hydrogen is highly dependent on the chosen computational methodology [14,15]. Moreover, it seems clear that no such critical point is ever present in α -C–H agostic bonds [16,17], suggesting that they may have a fundamentally different origin from their β counterparts. Indeed, Dobado and co-workers have argued that the term α -agostic ‘bond’ should be avoided, and replaced with ‘ α -agostic geometry’. Thus it seems that early transition metal agostic bonds are fundamentally different from their late transition metal analogues, and, moreover, that α -agostic bonds are fundamentally different from their β -agostic counterparts [18]. In view of the difficulties in pinpointing the origin of an agostic bond, a more pragmatic definition is generally adopted, based on their structural consequences. For example, Scherer et al. proposed the working definition that ‘agostic interactions are characterised by the distortion of an organometallic moiety which brings an appended C–H bond into close proximity with the metal centre’ [14]. In summary, although the manifestations of an agostic interaction have been known for almost 40 years, the driving force that lies behind the distortions remains poorly understood, and a number of complementary views have emerged in recent years. In this review we summarise our efforts over the past decade to understand the nature of agostic bonding in one particular class of system, the niobium alkyl complexes $Tp^{Me_2}NbCl(R'C\equiv CR'')(R)$ [19–24]. We also draw comparison with models proposed by other authors for early transition metal complexes, and argue that one common theme emerges: the structural distortion is not driven exclusively by direct interactions between C–H bonds and the metal centre, and reorganisation of the rather ionic metal–carbon bond can also play a role. The facial $Tp^{Me_2}M$ fragment provides a unique platform for agostic interactions, and leads to an unprecedented wealth of agostic behaviour within a closely related series of complexes. The niobium complexes $Tp^{Me_2}NbCl(R'C\equiv CR'')(R)$ clearly meet one of the principal criteria for agostic bonding, in so much as they are electron deficient (16e) species. The formal d^2 configuration of the Nb(III) centre means that one of the three low-lying orbitals on the metal (related to the octahedral t_{2g} set) is occupied, leaving two vacant orbitals which can, at least in principle, accept electron density from a ligand-based electron pair. However, as shown in the diagram in Fig. 1, one of these orbitals (d_{xz} in the figure) is poorly oriented to interact with the Nb– C_α bond, leaving only the Nb–Cl π^* orbital ($d_{x^2-y^2}$ in the figure) to accommodate an agostic interaction. This simple analysis of the electronic structure leads us to anticipate that agostic distortions will tend to force one substituent on the α carbon into the region of space bisecting the Cl–Nb– C_α angle (which we refer to as the ‘agostic position’). Moreover, donation of electron density from the C–H bond into the metal will be in direct competi-

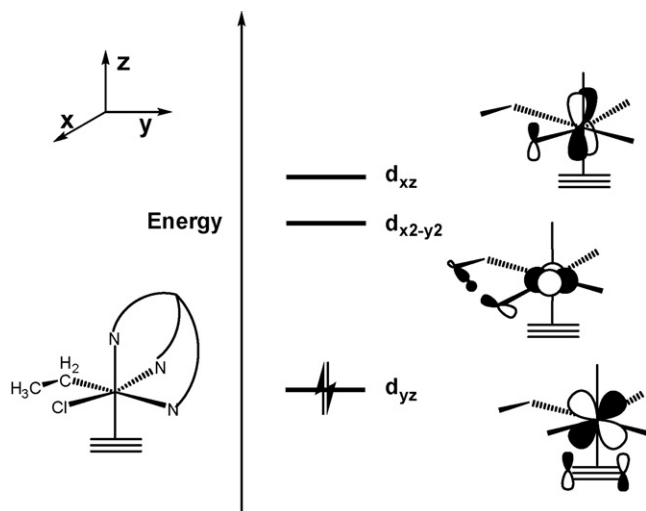


Fig. 1. Qualitative orbital diagram for $\text{TpNbCl}(\text{R}'\text{C}\equiv\text{CR}'')(\text{R})$ complexes. Only orbitals related to the octahedral t_{2g} set are shown.

tion with Nb–Cl π bonding, suggesting that the Nb–Cl bond length should be an indirect but sensitive probe of the agostic bond. In principle, then, any alkyl complex can adopt three distinct agostic conformations, differing only in the torsion angle about the Nb–C $_{\alpha}$ bond. For example, in the case of the isopropyl complex (Fig. 2), rotation of the alkyl moiety generates three distinct rotamers, **A**, **B** and **C**, which feature β -, α - and β -agostic alkyl interactions, respectively. In cases where both α - and β -CH bonds are available, β -agostic structures are almost always preferred over their α -agostic alternatives, suggesting that electronic factors favour the former. The unique feature of the $\text{Tp}^{\text{Me}_2}\text{NbCl}(\text{R}'\text{C}\equiv\text{CR}'')(\text{R})$ system is the presence of pendant methyl groups on the Tp^{Me_2} ligand, which define a tight steric pocket on the opposite face of the metal. As a result, there is a substantial barrier to rotation about the Nb–C $_{\alpha}$ bond, and isomers differing only in the torsion angles about this bond can form distinct well-defined minima on the potential

energy surface. In the case of secondary alkyls, this allows α - and β -CH agostic isomers to co-exist in dynamic equilibrium in solution, providing a unique opportunity to compare the two types of bond in an otherwise identical chemical environment. For example, in the isopropyl case shown in Fig. 2, rotamers **A** and **B** are in equilibrium in solution, but rotamer **C** is absent. The analysis of agostic behaviour in terms of these three rotamers is one of the foundations of this work, and will be used on several occasions in the following discussions.

Our work has involved a close interplay between synthesis, structural and spectroscopic characterization and analysis using density functional-based computational methods. In this review, we first summarise the experimental data for a broad range of complexes, where R can be either a cyclic or acyclic alkyl. We then report our efforts to understand these systems using theory, and illustrate how improvements in methodology over the past decade have allowed our model of agostic bonding to evolve.

2. Experimental data

In this section, we summarise the structural and spectroscopic data that constitute the foundation of this work. The results are organised according to the structure of the alkyl ligand, starting with simple primary and secondary alkyls and ending with their cyclic analogues. In this way, the complexity is seen to emerge logically as a function of chain length and structure.

2.1. Primary alkyl complexes

Despite their formally unsaturated nature, linear alkyl complexes of the type $\text{Tp}^{\text{Me}_2}\text{NbCl}(n\text{-C}_n\text{H}_{2n+1})(\text{R}_1\text{C}\equiv\text{CR}_2)$ ($n\text{-C}_n\text{H}_{2n+1} = \text{CH}_2\text{Me}, \text{CH}_2\text{CH}_2\text{Me}, \text{CH}_2\text{CH}_2\text{CH}_2\text{Me}$) ($\text{R}_1, \text{R}_2 = \text{Ph}, \text{Me}, \text{CH}_2\text{Me}, \text{CH}_2\text{CH}_2\text{Me}, \text{CF}_3, \text{H}$) (Chart 2), readily prepared from $\text{Tp}^{\text{Me}_2}\text{NbCl}_2(\text{R}_1\text{C}\equiv\text{CR}_2)$ and the appropriate Grignard reagent, are stable species at room temperature [19a].

The most immediately striking feature of the X-ray structures of $\text{Tp}^{\text{Me}_2}\text{NbCl}(\text{CH}_2\text{Me})(\text{PhC}\equiv\text{CCH}_2\text{Me})$ (the archetype with a linear alkyl ligand) and $\text{Tp}^{\text{Me}_2}\text{NbCl}(\text{CH}_2\text{SiMe}_3)(\text{PhC}\equiv\text{CMe})$ (Fig. 3) is

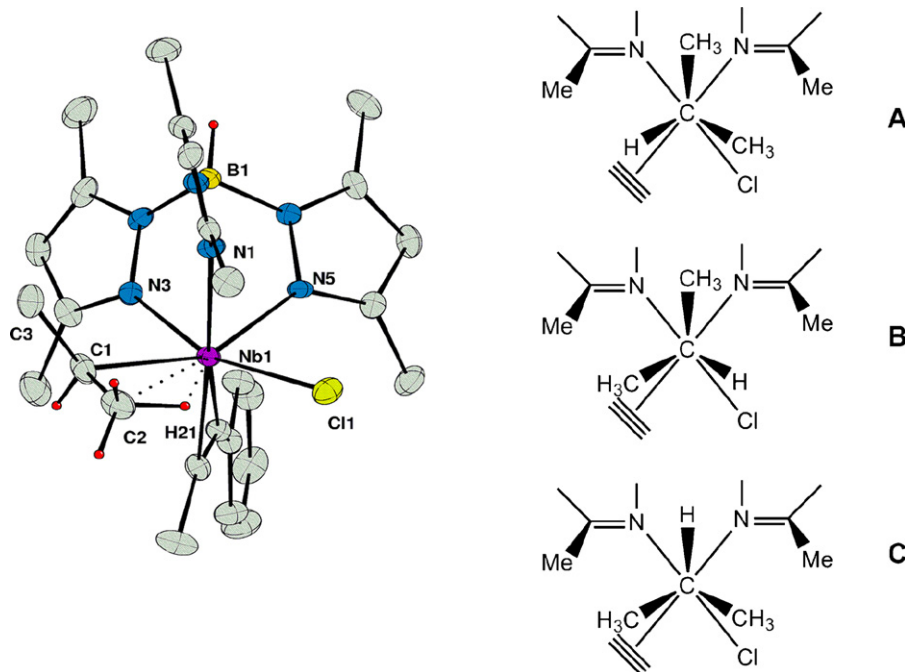


Fig. 2. Crystal structure of $\text{Tp}^{\text{Me}_2}\text{NbCl}(\text{PhC}\equiv\text{CMe})i\text{-Pr}$ (rotamer **A**) and the relationship between the rotamers (**A**–**C**) (viewed along the Nb–C $_{\alpha}$ bond).

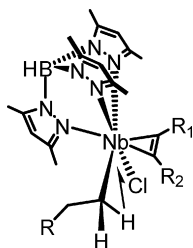


Chart 2. α -CH agostic primary alkyl complexes.

that both have an α -CH agostic distortion, despite the availability of alternative β (CH_2Me) or γ (CH_2SiMe_3) hydrogens. This offers the first indication that the Tp^{Me_2} ligand exerts a significant influence, overturning the usual preference for β -agostic structures over their α -agostic counterparts. The orientation of the ethyl and CH_2SiMe_3 chains away from the metal centre along a channel defined by two dimethylpyrazolyl groups is also common to both structures, and as a direct result, one of the two methylene hydrogens is forced into the 'agostic position' bisecting the $\text{Cl-Nb-C}\alpha$ angle. This analysis therefore suggests that the preference for an α -CH agostic interaction might be a consequence of the ethyl orientation rather than its cause. In the case of the CH_2SiMe_3 ligand, where data were of sufficient quality to allow location of the hydrogens, a distinct distortion at the α -carbon brings one hydrogen significantly closer to the metal centre than the other ($\text{Nb-C}\alpha\text{-H } 84(4)^\circ$, $\text{Nb}\cdots\text{H } 2.29(6)\text{ \AA}$; $\text{Nb-C}\alpha\text{-H } 113(3)^\circ$, $\text{Nb}\cdots\text{H } 2.67(4)\text{ \AA}$). The rather short Nb-Cl bond length of $2.4247(8)\text{ \AA}$ (*cf.* values of $\sim 2.49\text{ \AA}$ for the β -agostic systems, *vide infra*) does, however, suggest that whatever the nature of the interaction between metal and α -hydrogen, it does not weaken the Nb-Cl π bonding to the same extent.

The NMR spectra of these systems confirm that the preference for an α -C-H agostic structure persists in solution, and data for the ethyl complex $\text{Tp}^{\text{Me}_2}\text{NbCl}(\text{n-CH}_2\text{CH}_3)(\text{PhC}\equiv\text{CMe})$ serve to illustrate the diagnostic features of an α -C-H agostic interaction noted in the introduction: in the ^1H NMR spectrum, the ethyl protons appear as

an AM_3X type spectrum with δ 3.84 (dq, 1H, $J = 12.8, 7.8\text{ Hz}$), 1.15 (dd, 3H, $J = 7.8, 6.1\text{ Hz}$), 0.37 (pseudo sextet, 1H, $J = 12.8, 6.1\text{ Hz}$). The large difference in the chemical shifts of the diastereotopic methylene protons is remarkable, with the agostic proton being shielded whereas its diastereotopic companion is deshielded. In the ^{13}C NMR spectrum, the niobium bound carbon Nb-C α is a deshielded doublet of doublets with δ 86.5 (dd, $^1J_{\text{CH}} \approx 108, 129\text{ Hz}$). This lowering of $^1J_{\text{CH}}$ for the agostic CH bond is by far the most diagnostic signature of α -CH agostic bonding [1,2].

The accumulated structural and spectroscopic evidence for these primary alkyl complexes therefore clearly identifies them as rare cases where an α -CH agostic interaction is preferred over an apparently accessible β -CH agostic alternative. We have anticipated the role of pendant methyl groups in imposing this unusual situation, and we will use theory to analyse its origins in detail in the subsequent section. However, immediate experimental support for the critical role of the steric environment comes from the analogous reaction of ethylmagnesium chloride with the hydrotris(pyrazolyl)borate complex $\text{TpNbCl}_2(\text{PhC}\equiv\text{CMe})$, where the pendant groups are absent. The addition of one equivalent of ethylmagnesium chloride to $\text{TpNbCl}_2(\text{PhC}\equiv\text{CMe})$ at low temperature [25] gives an orange solution characteristic of the $\text{Tp}^{\text{Me}_2}\text{NbCl}(\text{alkyl})(\text{alkyne})$ complexes described above. However, the solution rapidly turned brown, and NMR analysis of the reaction mixture revealed extensive decomposition. The contrast with the Tp^{Me_2} analogue, which is stable under similar conditions, is striking: presumably the absence of steric hindrance in the Tp systems allows a β -CH agostic interaction to develop, ultimately leading to decomposition *via* β -H elimination. The strength of the agostic bond is also sensitive to other changes in the coordination sphere, and indeed replacing Cl by the better π -donor OMe in $\text{Tp}^{\text{Me}_2}\text{Nb}(\text{OMe})(\text{CH}_2\text{Me})(\text{PhC}\equiv\text{CMe})$ weakens the α -C-H agostic interaction. In the ^{13}C NMR spectrum, C α appears as a *triplet* with $^1J_{\text{CH}} = 116\text{ Hz}$ rather than a doublet of doublets down to 183 K, while in the ^1H NMR spectrum, the chemical shift difference for the diastereotopic methylene protons shrinks to 1.09 ppm with pseudo sextets for NbCHHMe (δ 1.60, $J = 14.0, 7.0\text{ Hz}$) and NbCHHMe (δ 2.69, $J = 14.0, 7.0\text{ Hz}$) [19b].

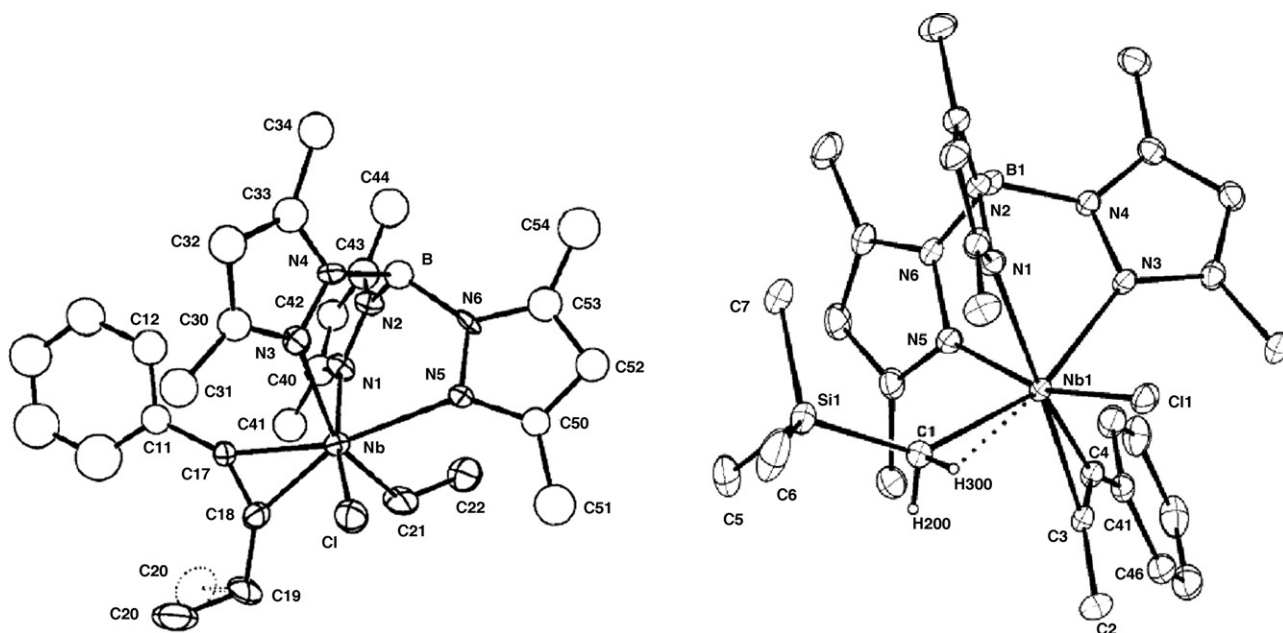


Fig. 3. Plots of the X-ray molecular structures of $\text{Tp}^{\text{Me}_2}\text{NbCl}(\text{CH}_2\text{Me})(\text{PhC}\equiv\text{CCH}_2\text{Me})$ (left) and $\text{Tp}^{\text{Me}_2}\text{NbCl}(\text{CH}_2\text{SiMe}_3)(\text{PhC}\equiv\text{CMe})$ (right).

2.2. Acyclic secondary alkyl complexes

The notion that steric interactions might play a decisive role in orienting the chain and hence promoting the α -CH agostic interaction in primary alkyl complexes prompted us to explore their bulkier secondary alkyl analogues [20,21]. We first focussed on the simplest secondary alkyl group, *i*-Pr, and then turned to the *sec*-butyl analogue, where the chirality at both the niobium centre and the α carbon results in the isolation of two distinct diastereomers, labelled **AR-CS** and **CR-AS**. The X-ray crystal structures of all three complexes are shown in Fig. 4.

The most striking structural feature is that all three adopt β -CH agostic structures, in stark contrast to the α -agostic structures adopted by their primary alkyl complexes analogues. The agostic group again lies in the $C\alpha$ -Nb-Cl plane, and the β -agostic interaction is characterised by short Nb-C β distances [2.608(4) Å – 2.789(5) Å] and small Nb-C α -C β angles [87.0(3)° – 95.3(3)°]. The $C\alpha$ -C β bond (*ca* 1.48 Å) for the agostic β -carbon is also significantly shorter than that for the non-agostic β -carbon (*ca* 1.52 Å) in all three cases, indicating some double bond character. The adoption of a β -agostic structure necessarily brings a rather bulky methyl or ethyl group into the niobium coordination sphere, and this has a significant impact on the rest of the structure, most notably the Nb-Cl bond lengths which, at *ca* 2.49 Å, are some 0.07 Å longer than those in the α -agostic analogues shown in Fig. 3. This contrast suggests a fundamental difference between α -CH and β -CH agostic interactions – the latter appear to weaken the Nb-Cl bond to a far greater extent than the former. We will return to this important point in subsequent sections.

The NMR spectroscopy of the isopropyl complex, along with one of the two diastereomers of the *sec*-butyl complex (**AR-CS**), proved to be quite remarkable – both show clear evidence for an unprecedented equilibrium between the dominant β -CH agostic rotamer (observed in the solid-state), **A** in Fig. 2, and a minor α -CH agostic rotamer, **B** (Chart 3). The presence of a dynamic equilibrium between α - and β -CH agostic structures is quite remarkable, and has, to the best of our knowledge, only been observed in one other instance – a tantalum complex where the thermodynamic parameters were quite different [26]. The detailed analysis of the spectra leading to either β -CH or α -CH assignments can be found in the original paper [21].

The putative third rotamer, **C**, with the α -hydrogen in the wedge and a methyl group in the $C\alpha$ -Nb-Cl plane was *not* detected. The equilibrium constant at 193 K, K_{193} , is 4.0, indicating that the β -CH agostic rotamer **A** is favoured, and analysis of the temperature-dependence of this equilibrium indicates that the origin of this preference is enthalpic ($\Delta H^0 = -7.4$ kJ mol $^{-1}$) rather than entropic ($\Delta S^0 = -27$ J mol $^{-1}$ K $^{-1}$). The spectroscopic properties of the **AR-CS** diastereoisomer of $\text{Tp}^{\text{Me}_2}\text{NbCl}(\text{sec-Bu})(\text{MeC}\equiv\text{CMe})$ are remarkably similar to those of the isopropyl complex, again indicating the presence of an equilibrium between β -CH and α -CH-agostic rotamers (Chart 3). In stark contrast, the other diastereoisomer, **CR-AS**- $\text{Tp}^{\text{Me}_2}\text{NbCl}(\text{sec-Bu})(\text{MeC}\equiv\text{CMe})$ shows no evidence of any dynamic behaviour, and only the β -agostic structure observed in the solid state is present in solution.

In the discussion of the primary alkyl complexes, we noted that in each case the bulkiest substituent on the α -carbon was directed along a channel between two of the pendant methyl groups of the Tp^{Me_2} , thus minimising any steric clash. Furthermore, we argued that the driving force favouring this orientation outweighs the intrinsic electronic preference for β -agostic interactions, thus enforcing the α -agostic alternative. Although β -agostic structures dominate in all three secondary alkyl systems, their dynamic behaviours clearly reflect this competition between steric and electronic effects. In the *i*-Pr case, both α - and β -agostic rotamers (**A** and **B**) satisfy the steric requirements by placing a methyl group in the sterically least demanding position along the wedge. This then leaves a choice of H or CH_3 groups to occupy the agostic position bisecting the $C\alpha$ -Nb-Cl angle, and the presence of both in solution suggests that precise nature of the agostic interaction is less important, in energetic terms, than the steric demands. Consistent with this, the putative third rotamer, which would place the smallest substituent (H) at the α carbon along the wedge, thereby introducing unfavourable steric clashes elsewhere, is not observed. In the **AR-CS** diastereoisomer of the *sec*-Bu complex, the most favourable situation in terms of sterics, with the largest substituent at the α -carbon (CH_2CH_3) in the least sterically demanding position along the wedge, necessarily places the α -C-H group in the agostic position. The electronically favoured β -C-H agostic structure, in contrast, necessarily places the smaller CH_3 group along the wedge, and so the position of the equilibrium

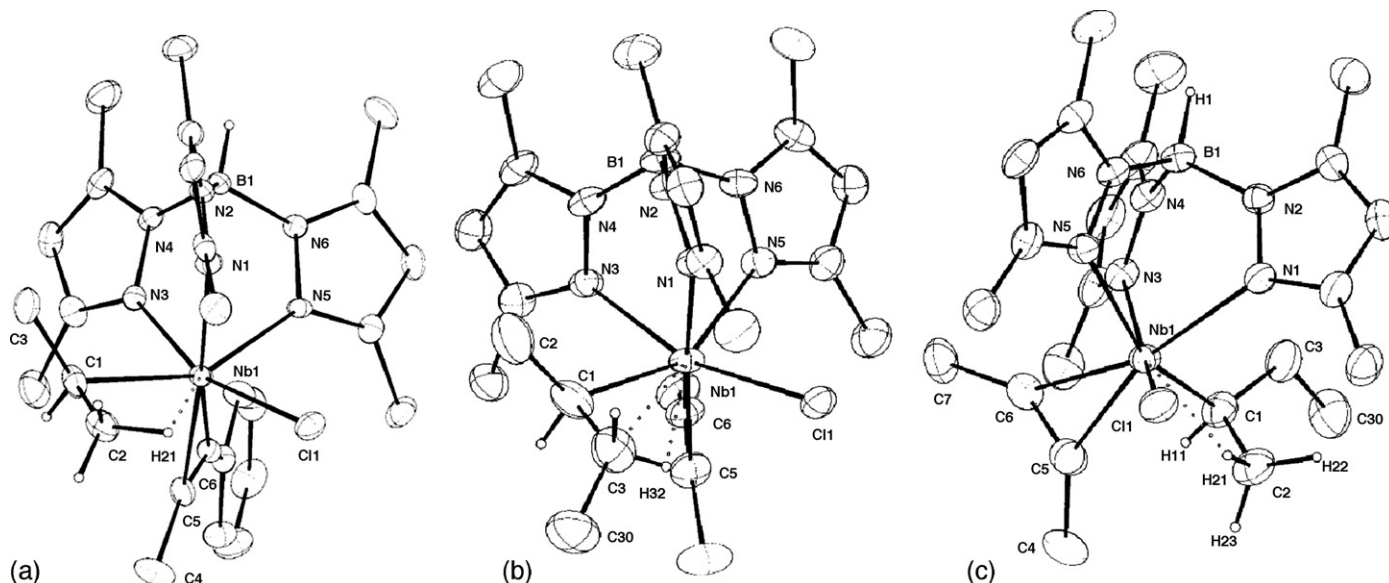


Fig. 4. Plots of the X-ray molecular structures of (a) $\text{Tp}^{\text{Me}_2}\text{NbCl}(\text{i-Pr})(\text{PhC}\equiv\text{CMe})$, (b) **AR-CS**- $\text{Tp}^{\text{Me}_2}\text{NbCl}(\text{sec-Bu})(\text{MeC}\equiv\text{CMe})$ and (c) **CR-AS**- $\text{Tp}^{\text{Me}_2}\text{NbCl}(\text{sec-Bu})(\text{MeC}\equiv\text{CMe})$.

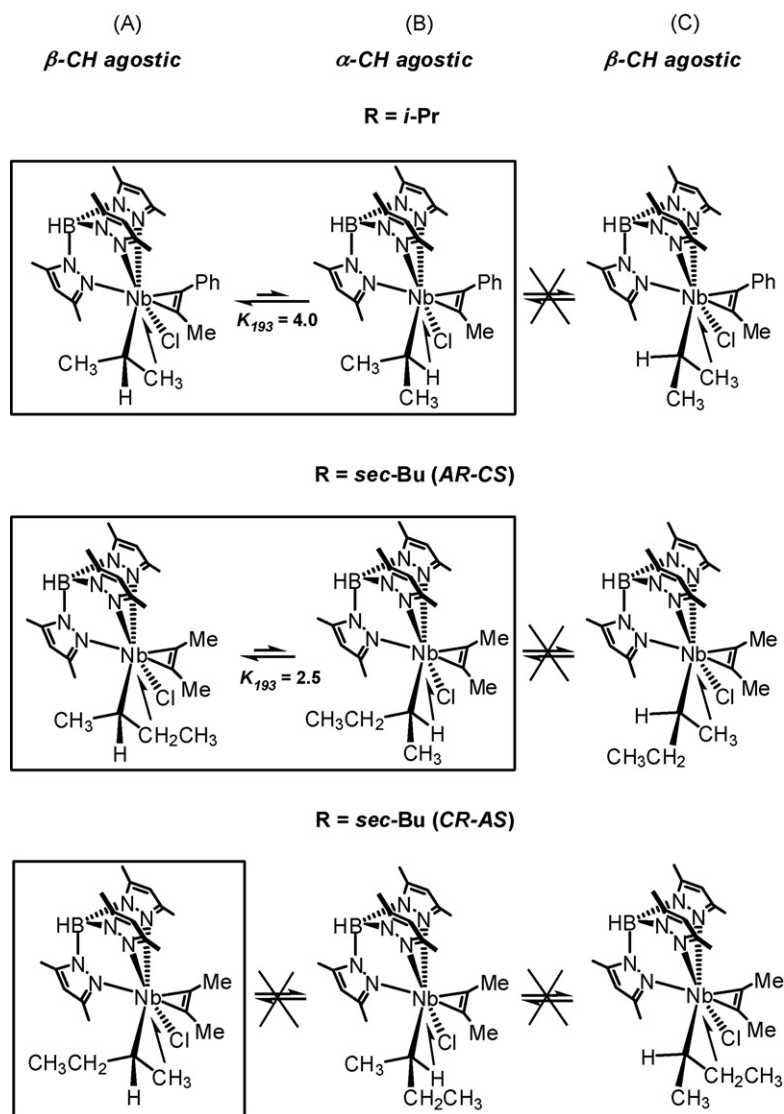


Chart 3. Equilibria between agostic rotamers in secondary alkyl complexes.

reflects a compromise between steric and electronic driving forces. In contrast, the β -agostic structure of the **CR-AS** diastereoisomer involves no such compromise: the adoption of an electronically favourable β -agostic structure naturally aligns the large CH_2CH_3 group along the wedge, so steric and electronic requirements are satisfied simultaneously. As a result, both alternative rotamers (**B** and **C**) are strongly destabilised, and neither is observed experimentally.

In the previous paragraphs we have concentrated solely on the thermodynamic aspects of the exchange of α - and β -agostic isomers, but spin saturation transfer experiments at different temperatures also provide access to kinetic parameters for the interconversion of the β -CH and α -CH agostic rotamers, and high barriers are observed for both $\text{Tp}^{\text{Me}_2}\text{NbCl}(i\text{-Pr})(\text{MeC}\equiv\text{CMe})$ ($\Delta H^\ddagger = 58.8 \pm 2.5 \text{ kJ mol}^{-1}$, $\Delta S^\ddagger = 59 \pm 10 \text{ J mol}^{-1} \text{ K}^{-1}$) and for **AR-CS**- $\text{Tp}^{\text{Me}_2}\text{NbCl}(\text{sec-Bu})(\text{MeC}\equiv\text{CMe})$ ($\Delta H^\ddagger = 56.0 \pm 2.5 \text{ kJ mol}^{-1}$, $\Delta S^\ddagger = 75 \pm 10 \text{ J mol}^{-1} \text{ K}^{-1}$). The positive entropies of activation point to a less ordered transition state in which the agostic interaction is lost (i.e. a dissociative process), and the enthalpy of activation ΔH^\ddagger of ca 60 kJ mol^{-1} defines an *upper* limit for the strength of these agostic interactions [21].

2.3. Cyclic (secondary) alkyl complexes

Cyclic ligands are in principle simply secondary alkyl groups, the major difference between them and their acyclic counterparts being the reduced conformational freedom of the two substituents at the α carbon as a result of their position in a ring. For ring sizes between C_4 and C_6 [$\text{Tp}^{\text{Me}_2}\text{NbCl}(c\text{-C}_n\text{H}_{2n-1})(\text{MeC}\equiv\text{CMe})$ ($n = 4, 5, 6$)] [23–25], the situation is in fact rather similar to the *i*-Pr and *sec*-Bu cases, with an equilibrium between α - and β -agostic rotamers again established in solution. The speciation in solution is, however, subtly different, with the α -CH agostic rotamers dominating in all three cases. This preference also extends to the solid state, where X-ray data confirm the presence of an α -agostic interaction: the X-ray structure of a representative example, the cyclopentyl complex $\text{Tp}^{\text{Me}_2}\text{NbCl}(c\text{-C}_5\text{H}_9)(\text{MeC}\equiv\text{CMe})$ (Fig. 5) shows the short Nb–C α and Nb–Cl bonds (2.174(4) and 2.430(1) Å, respectively) typical of the α -agostic structures of the primary alkyls. The (located and refined) agostic hydrogen lies in the Cl–Nb–C α plane, 2.21(4) Å from Nb. The C β –C α –C β' angle of $104.4(4)^\circ$ is virtually equal to other C–C–C angles within the ring indicating no distortion around C α . The ^1H NMR spectrum confirms the presence of a vastly dominant α -CH

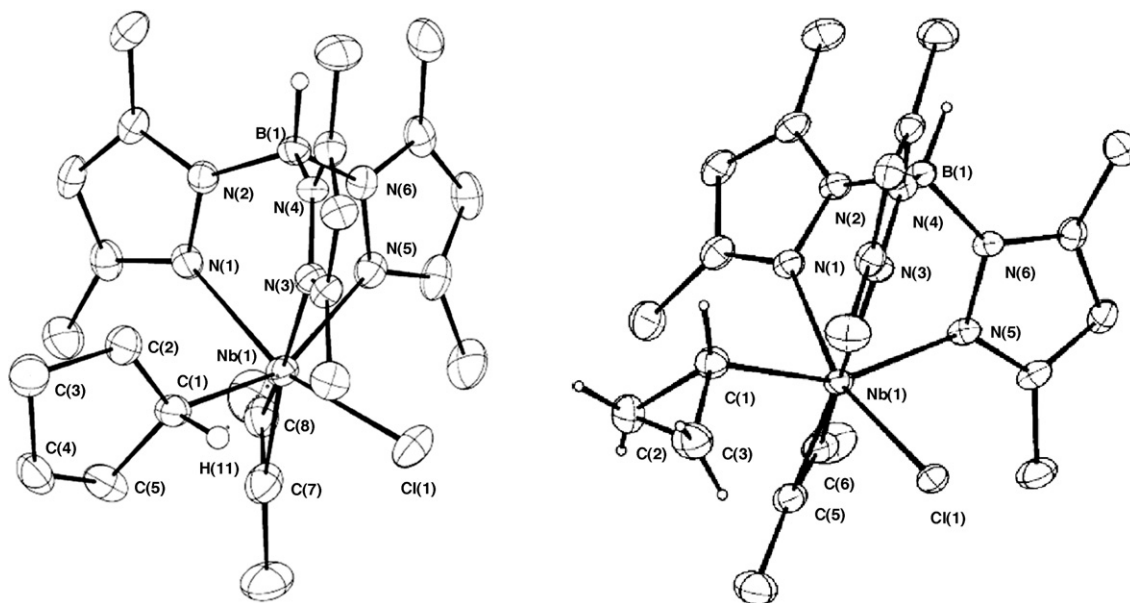


Fig. 5. Plots of the X-ray molecular structures of $\text{Tp}^{\text{Me}_2}\text{NbCl}(\text{c-C}_5\text{H}_9)(\text{MeC}\equiv\text{CMe})$ (left), and $\text{Tp}^{\text{Me}_2}\text{NbCl}(\text{c-C}_3\text{H}_5)(\text{MeC}\equiv\text{CMe})$ (right).

agostic rotamer (a shielded signal at $\delta -0.93$ correlates with a ^{13}C NMR doublet at $\delta 135.8$ with $^1J_{\text{CH}} = 93$ Hz). The cyclohexyl complex $\text{Tp}^{\text{Me}_2}\text{NbCl}(\text{c-C}_6\text{H}_{11})(\text{MeC}\equiv\text{CMe})$ also shows dynamic behaviour in solution, with a major α -CH agostic rotamer in equilibrium with a second isomer ($K_{183} = 11.0$) which may or may not be β -CH agostic. The thermodynamic data therefore suggest that although the α -agostic rotamer dominates in all cases, its stability relative to the β -agostic rotamer decreases as the ring size increases. The structures of the β -agostic rotamers of the secondary alkyls (Fig. 4) offer an important clue to the origin of the difference between acyclic and cyclic complexes. In the *i*-Pr structure, one methyl group is fixed in place by an agostic interaction while the other is locked by the steric bulk of the pendant methyl groups, and this simultaneous locking of both groups forces the $\text{C}\beta\text{--C}\alpha\text{--C}\beta$ angle to open up to 119° . In the α -agostic rotamers, in contrast, only one of the two methyl groups is locked in place (by the pendant methyl groups), and so the $\text{C}\beta\text{--C}\alpha\text{--C}\beta$ angle is not required to open up to the same extent (there are no X-ray data available for the α -agostics to confirm this argument, but calculations show that the angles are close to 109° in all cases – *vide infra*). The major difference between cyclic and acyclic secondary alkyl groups is that the $\text{C}\beta\text{--C}\alpha\text{--C}\beta$ angles in the former are less flexible as a consequence of being part of a ring, and it is the inability to open up this angle that destabilises the β -agostic structure relative to its α -agostic counterpart. This subtle but important difference is sufficient to switch the dominant isomer in solution from β -agostic in the acyclic species to α -agostic in their cyclic analogues.

2.4. Cyclopropyl complexes: a rare example of an α -CC agostic interaction

The structural and spectroscopic properties of the cyclopropyl derivatives $\text{Tp}^{\text{Me}_2}\text{NbX}(\text{c-C}_3\text{H}_5)(\text{MeC}\equiv\text{CMe})$ ($\text{X} = \text{Cl}, \text{Br}$) indicate that these species are fundamentally different in nature from their larger ring analogues [22,23]. Most conspicuously, there is no evidence for either an α -CH or β -CH agostic interaction of any kind – a rather surprising observation in light of the ubiquitous presence of these interactions in all other alkyl complexes. Thus in the ^{13}C NMR spectrum, Nb–C α H appears as a broad doublet at $\delta 75.3$ (d, $^1J_{\text{CH}} 139$ Hz) and C β and C β' appear as triplets at $\delta 13.8$ and 3.2

($^1J_{\text{CH}} 159$ Hz). In the X-ray structure (Fig. 5), the cyclopropyl group is oriented such that one of the C α –C β bonds occupies the agostic position bisecting the C α –Nb–Cl angle. Although the Nb...C β separation is rather long, the C(1)–C(3) bond is significantly longer than the other two (1.539(4) Å vs 1.490(4) Å and 1.478(5) Å). The contrast with the β -CH agostic *i*-Pr complex, where the C–C bond in the agostic position is shorter than its non-agostic counterpart, is particularly striking. The computational work summarised in the following sections offers further support for our proposal of a C–C, rather than C–H, agostic structure in this cyclopropyl complex.

3. Hybrid DFT/MM studies

The results presented in the previous section provide an exciting picture of the diversity of agostic interactions attainable using the $\text{Tp}^{\text{Me}_2}\text{Nb}$ platform, but the experiments alone are unable to offer a complete understanding of the phenomenon. For example, full characterization of the various compounds is often difficult to achieve, particularly in the case of minor isomers, the presence of which can be deduced only from NMR spectra. Thus theory has an important role to play in predicting structures of species that remain inaccessible to diffraction experiments.

Our analysis in the previous section is based largely on the qualitative concept of competing steric and electronic effects. Hybrid DFT/MM techniques, where a part of the system is described with an accurate DFT method and the rest with a force field, provides an ideal framework for quantifying these ideas. If one accepts the usual assumption that the steric effects of the MM region are properly introduced, but their electronic effects are neglected [27,28], then DFT/MM calculations allow a clear separation of sterics from electronics. More pragmatically, hybrid techniques such as this were the only viable option at a reasonable computational cost when this collaboration started in 1998. In this section, we describe how theory complemented experiment to develop our understanding of these systems. We have subsequently re-evaluated our model using full DFT calculations, with some surprising results that will be the subject of the final section of this review.

The partition used in our hybrid QM/MM study is shown in Fig. 6. The tris(pyrzoyl) ligand is substantially simplified and some electronic effects are obviously neglected, but this approach has proved

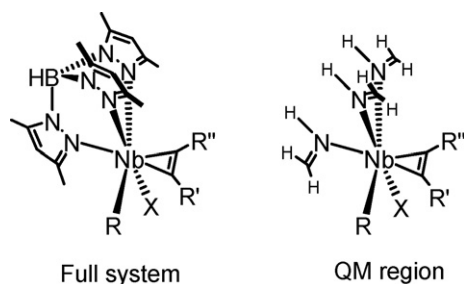


Fig. 6. The QM/MM partition used in the studies of the $\text{Tp}^{\text{Me}_2}\text{NbX}(\text{R})(\text{R}'\text{CCR}'')$ systems.

to give a reasonable qualitative picture for other systems [29]. Slightly different QM/MM approaches IMOMM(B3LYP:MM3) [30] and ONIOM(B3LYP:UFF) [31] were applied over the course of this work, largely reflecting the ongoing development of commercial codes. The results are slightly different, mainly as a consequence of the nature of the force field, but these slight differences do not have any bearing on our interpretation.

Our earliest work focussed on the acyclic alkyls, $\text{Tp}^{\text{Me}_2}\text{NbCl}(\text{CH}_2\text{Me})(\text{PhC}\equiv\text{CCH}_2\text{Me})$ and $\text{Tp}^{\text{Me}_2}\text{NbCl}(i\text{-Pr})(\text{PhC}\equiv\text{CCH}_2\text{Me})$, which were first investigated using the IMOMM(B3LYP:MM3) method [20]. Only one minimum was located for the ethyl complex, corresponding to the structurally characterised α -agostic isomer [19b]. In contrast, two distinct minima were obtained for the isopropyl complex, fully consistent with the experimental data. One of these corresponds to the experimentally isolated β -agostic structure, while the other, 9.3 kJ mol^{-1} higher in energy, is an α -agostic isomer related to the first by rotation of 120° about the $\text{Nb}-\text{CH}(\text{CH}_3)_2$ bond. The computed energetic separation is in excellent agreement with the experimental value (ΔH) of 7.4 kJ mol^{-1} . All three structures showed features typical of agostic interactions: $\text{Nb}\cdots\text{H}$ distances were quite short ($2.35\text{--}2.58 \text{ \AA}$), the $\text{C}-\text{H}$ agostic bonds were elongated ($1.112\text{--}1.116 \text{ \AA}$), the $\text{Cl}-\text{Nb}-\text{C}\alpha$ angles were wide ($110.8\text{--}126.9^\circ$) and the angles between the $\text{Nb}-\text{C}\alpha$ bond and the agostic group were narrow ($86.3\text{--}92.4^\circ$). The geometrical parameters associated with the position of the hydrogen atom, in particular the $\text{C}-\text{H}$ distance, are particularly diagnostic for agostic interactions, but, as noted above, are very difficult to obtain from X-ray diffraction, because the small elongation (a few hundredths of \AA) is well within experimental error.

Computational experiments on hypothetical systems generated by modification of the experimental complexes have proved invaluable in assessing the competition between steric and electronic effects. For example, calculations on the $\text{Tp}^{5\text{-Me}}\text{NbCl}(\text{CH}_2\text{Me})(\text{PhC}\equiv\text{CCH}_2\text{Me})$ system, where $\text{Tp}^{5\text{-Me}}$ is the hypothetical hydridotris(5-methylpyrazolyl)borate ligand, differing from Tp^{Me_2} only in the absence of the methyl groups in the 3 position, offer the opportunity to identify the dominant agostic interactions in the absence of steric pressure. Only a single stable rotamer was located for the Tp^{Me_2} system, and the same is true with $\text{Tp}^{5\text{-Me}}$, but it is not the same rotamer! When the ligand is Tp^{Me_2} the most stable structure is the α $\text{C}-\text{H}$ agostic rotamer **B** (Fig. 2), in good agreement with experiment. However, for $\text{Tp}^{5\text{-Me}}$, the structure collapses to β $\text{C}-\text{H}$ agostic rotamer **A**. The preference for the α $\text{C}-\text{H}$ agostic structure over its β $\text{C}-\text{H}$ agostic counterpart can be thus traced directly to the steric constraints imposed by the Tp^{Me_2} ligand. Repulsions between Tp^{Me_2} and the alkyl chain are clearly minimised when the largest substituent on the α carbon is aligned between two pendant Me groups, forcing one of the α hydrogens to lie in the agostic position. In the absence of these pendant methyls, the system reverts to the electronically favoured β $\text{C}-\text{H}$ agostic structure.

For the cyclic systems, computed structures and energies are again in excellent agreement with experiment: for the cyclopentyl system, the α -CH agostic rotamer **B** was more stable than its β -agostic counterpart (**A**), and the elongation of the $\text{C}-\text{H}$ bond in the former (1.12 \AA) was consistent with a substantial α $\text{C}-\text{H}$ agostic interaction [23]. Furthermore, the close energetic proximity of rotamers **B** and **A** in this case allowed us to identify the latter as the most likely candidate for the minor isomer observed in solution. We argued in the previous section that the relative instability of the β -agostic structure in cyclic systems was a consequence of a constraint placed on the $\text{C}\beta-\text{C}\alpha-\text{C}\beta$ angle, which prevented the system from simultaneously attaining the optimal steric and electronic geometries. When the pendant methyl groups are removed ($\text{Tp}^{5\text{-Me}}$), we find that the relative stabilities of **A** and **B** are reversed, with the β -agostic rotamer now preferred. These computational experiments therefore confirm that the constraints imposed by the cyclic ring prevent the alkyl ligand from adapting to the well-defined steric environment of the Tp^{Me_2} ligand, and force it to adopt an electronically less favourable but sterically preferred α -CH agostic alternative. The analysis of the relative stabilities of the different rotamers of the cyclobutyl system [24] follows the same lines.

The remarkable structure of the cyclopropyl complex $\text{Tp}^{\text{Me}_2}\text{NbCl}(c\text{-C}_3\text{H}_5)(\text{MeC}\equiv\text{CMe})$ described in the previous section poses a number of challenges to theory. The orientation of the cyclopropyl group places one of the CH_2 groups of the 3-membered ring in the agostic position, and so, in principle a β $\text{C}-\text{H}$ agostic interaction could result. This is the case for the straight chain alkyl complexes, where the opening of the $\text{Cl}-\text{Nb}-\text{C}\alpha$ angle and the tilting of the alkyl group bring the $\text{C}-\text{H}$ bond into the $\text{C}\alpha-\text{Nb}-\text{Cl}$ plane. The first structural feature is certainly present in the cyclopropyl complex ($\text{Cl}-\text{Nb}-\text{C}$ angle of 110.9°) but neither ^1H nor ^{13}C NMR data support the presence of $\text{C}-\text{H}$ agostic interactions. The absence of agostic $\text{C}-\text{H}$ interactions was confirmed by our theoretical ONIOM(B3LYP:UFF) study, where we again computed all three rotamers, **A**, **B** and **C**, shown in Fig. 2. Consistent with experiment, but in contrast to all other cases, the most stable is rotamer **C**, where the $\text{C}1-\text{C}3$ bond is in the agostic site. The relative stability of rotamer **C** suggests that steric factors are less important in this case than in any of the other alkyls, cyclic or acyclic, and indeed removal of the steric bulk (by using the $\text{Tp}^{5\text{-Me}}$ ligand) does not alter the order. The lower steric pressure in the cyclopropyl case is a reflection of the smaller effective size of the alkyl substituent: the acute $\text{C}\beta-\text{C}\alpha-\text{C}\beta$ angle draws the β carbons away from the pendant methyl groups in rotamer **C**, hence stabilising this conformation relative to **A** or **B**.

The key features of the X-ray structure shown in Fig. 5 are well reproduced, most notably the long $\text{C}1-\text{C}3$ bond (calculated, 1.55 \AA ; X-ray, 1.539 \AA). This elongation of the $\text{C}-\text{C}$ bond is distinct from the contraction typically observed in β - $\text{C}-\text{H}$ agostic systems, and strongly suggests that it is the $\text{C}-\text{C}$, rather than the $\text{C}-\text{H}$, bond that is donating into the metal fragment. Moreover, calculations confirm that there is no elongation whatsoever of any of the $\text{C}-\text{H}$ bonds, effectively eliminating a $\text{C}-\text{H}$ agostic interaction. It thus appears that in this cyclopropyl complex the α $\text{C}-\text{C}$ bond is more nucleophilic than its β $\text{C}-\text{H}$ counterpart. One possible cause of this unusual behaviour is the acute angles in the 3-membered ring, which necessarily cause a rehybridisation at the α carbon and destabilisation of the $\text{C}-\text{C}$ σ bonds. To address this issue we performed a further computational experiment where the cyclopropyl group was replaced by an ethyl ligand whose bond angles and torsions were constrained to replicate those in cyclopropane [22]. In the unconstrained ethyl system, only rotamer **B**, an α -CH agostic structure, corresponds to a minimum but when the constraints are applied rotamer **A** is strongly stabilised, to the extent that it lies 21 kJ mol^{-1} below any other. Moreover, the $\text{C}\alpha-\text{C}\beta$ bond is signif-

icantly elongated, confirming that it is the acute $\text{C}\beta\text{--C}\alpha\text{--C}\beta$ bond angle that forces the $\text{C}\alpha\text{--C}\beta$ bond to participate into the agostic interaction in preference to the $\beta\text{--C--H}$ bonds.

4. The electronic origin of agostic interactions

The hybrid DFT/MM calculations summarised in the previous paragraphs have offered significant insights into the complex agostic equilibria exhibited by these systems. In particular, the methodology offers a transparent approach to separating steric and electronic effects, and has clearly highlighted the pivotal role of the pendant methyl groups in controlling the metal coordination sphere. Thus far, however, we have focussed on the *consequences* of agostic interactions (i.e. the distortion of the alkyl framework) rather than their underlying *cause*. As noted in the introduction, the latter has been the cause of spirited debate in the recent literature, driven by the development of tools such as the atoms in molecules (AIM) approach [11] which promise to deliver new insights into chemical bonding. The final section in this review describes our very recent attempts to explore the electronic mechanisms that underpin these 'agostic' interactions.

A pre-requisite for an analysis of the electron density is naturally a very accurate description of the electronic structure around the metal centre. Although the agreement between the hybrid DFT/MM theory described above and experiment was in most cases encouraging, there were some worrying discrepancies in the structural data. The most notable of these was in the Nb–Cl bond length, which was significantly underestimated in the $\beta\text{--CH}$ agostic structures, by as much as 0.128 Å in the IMOMM(B3LYP:MM3) study of $\text{Tp}^{\text{Me}_2}\text{NbCl}(\text{CH}_2\text{Me})(\text{PhC}\equiv\text{CCH}_2\text{Me})$ [20]. Discrepancies between experiment and DFT/MM are usually attributed to the neglect of the electronic influence of atoms in the MM region, and we therefore decided to repeat some of the calculations using a full DFT (B3LYP) protocol to describe the whole molecule, in the expectation that this would improve agreement with experiment and provide a more accurate electron density. Our chosen test case was the *i*-Pr complex, where the availability of both $\alpha\text{--}$ and $\beta\text{--CH}$ agostic structures offers an opportunity to explore fundamental differences between these two types of interaction. The results, summarised in Table 1, tell a rather different story: including the whole molecule within the QM partition does not result in an improved geometric description of the $\beta\text{--CH}$ agostic structure, but rather a much worse one! [32]. The $\beta\text{--CH}$ bond moves out of the niobium coordination sphere entirely, and the Nb–Cl bond length remains far shorter than the experimental value. For the $\alpha\text{--CH}$ agostic structure, in contrast, the move to a full-QM description causes less dramatic changes, and the C–H bond remains close to the metal centre. We have highlighted on several occasions the fact that agostic and Nb–Cl π bonding are in direct competition for vacant orbital space on the metal centre, and it appears that, at least for the $\beta\text{--CH}$ agostic rotamer, the B3LYP functional fails to accurately describe the balance between these two factors.

A wider survey of commonly used density functionals showed that the failure to locate a $\beta\text{--CH}$ agostic minimum was common to all cases where the LYP functional was used to describe the cor-

relation part. In contrast, the GGA functional PBE1PBE (along with many others) does reproduce the $\beta\text{--CH}$ agostic geometry, while at the same time providing a much improved description of the Nb–Cl bond length. The very different behaviour of these two functionals can be linked to the approximations used to generate the correlation functionals, and in particular their relationship to the uniform electron gas (UEG) approximation. In the local density approximation (LDA) the exchange and correlation energies of a system at a given point in space are assumed to be those of a homogeneous electron gas of uniform density at that point. Consequently, the LDA performs well for uniform or slowly varying densities, but is less reliable in molecular systems where rapid density variations are the norm. This deficiency is addressed by generalised gradient approximation (GGA) functionals such as PBE1PBE, which are usually constructed as corrections to the LDA using terms that depend on the gradients of the density. The LYP correlation functional, in contrast, was not formulated as a correction of LDA, but was instead constructed by recasting the Colle–Salvetti correlation energy formula of the helium atom [33] in terms of gradient expansions. LYP does not, therefore, adhere to the uniform electron gas (UEG) limit. In our survey of functionals we note a clean separation: only functionals that adhere to the UEG limit locate a $\beta\text{--CH}$ agostic minimum. By extension, we can conclude that a correct description of a $\beta\text{--agostic}$ bond requires an accurate description of a slowly varying region of electron density – precisely the situation we might anticipate in the region between a C–H bond and a metal centre. The structure of the $\alpha\text{--CH}$ agostic, in contrast, is rather insensitive to functional, suggesting that an accurate description of the region between the C–H bond and the metal is not, in this case, critical. This observation offers further evidence that the $\alpha\text{--agostic}$ and $\beta\text{--agostic}$ interactions are fundamentally different in nature.

Having established that non-UEG correlation functionals are poorly suited to describing the agostic interactions in this class of systems, a natural question to ask is why we obtained such apparently good results using this functional in our original hybrid DFT/MM calculations. The answer is that the simplifications inherent in our chosen QM/MM partitioning introduced artifacts that compensated for the intrinsically poor description offered by the B3LYP functional. The most obvious of these is the modelling of an anionic Tp^{Me_2} ligand with three neutral imine groups (Fig. 6), which introduces a net positive charge in the QM partition. An additional but unphysical electrostatic interaction between the metal centre and the alkyl ligand therefore draws the $\beta\text{--CH}$ bond into an agostic position, but without truly capturing the essence of the agostic interaction. In fact the short Nb–Cl bond in the DFT/MM calculations provides the clearest indication that the bonding is not being properly described: the optimised structure at this level apparently indicates the presence of *both* a $\beta\text{--CH}$ agostic interaction and a strong Nb–Cl π bond – a situation that is incompatible with the competition between these two donors for a single orbital (Fig. 1).

The above discussion highlights a very important point: optimised structural parameters, particularly those associated with an easily deformable group like an alkyl ligand, provide a rather poor criterion on which to judge the quality of the underlying description of electronic structure. Experimentalists rely on NMR parameters,

Table 1
Structural parameters for the $\alpha\text{--}$ and $\beta\text{--agostic}$ rotamers of $\text{Tp}^{\text{Me}_2}\text{NbCl}(\text{MeC}\equiv\text{CMe})(\text{CH}(\text{CH}_3)_2)$ (angles in degrees, distances in Å, relative energies in kJ mol^{-1})

	$\beta\text{--agostic}$ rotamer						$\alpha\text{--agostic}$ rotamer				
	NbC α C β	Nb–C β	Nb–H β	C β –H	C β –H'	Nb–Cl	NbC α H α	Nb–C α	Nb–H α	C α –H	Nb–Cl
Expt.	87.0(3)	2.608(4)	2.17(5)	1.11(5)		2.493(1)					
B3LYP/UFF	90.7	2.73	2.37	1.11	1.09	2.43	85.2	2.22	2.38	1.10	2.43
B3LYP	109.3	3.15	3.23	1.09	1.09	2.44	86.0	2.26	2.45	1.11	2.46
PBE1PBE	87.2	2.62	2.20	1.12	1.09	2.49	84.4	2.23	2.39	1.11	2.44

notably $^1J_{C-H}$, as their primary measure of agostic bonding, the changes in this coupling constant being indicative of weakening of the agostic C–H bond itself or of rehybridisation of the carbon atoms in the alkyl backbone. In a recent paper [34] we computed these coupling constants for both α - and β -CH agostic isomers of the *i*-Pr system, and showed a remarkable convergence of experiment and theory. This, in combination with excellent prediction of structural and energetic parameters, gives us real confidence that, in contrast to previous DFT/MM calculations, our full QM approach using the PBE1PBE functional is capturing the essential physics of the agostic interaction. The converged wavefunctions and electron densities that emerge from these calculations therefore provide a solid foundation on which to build a conceptual model of the agostic bond.

We noted in the introduction the controversy surrounding the interpretation of BCPs in electron density plots for agostic systems. Popelier has argued that the presence of such a BCP between the metal and the β hydrogen was indicative of a β -C–H agostic bond in $[(C_2H_5)_3TiCl_2]^+$ [13], while Scherer and co-workers have shown that their presence or absence is highly dependent on the chosen computational methodology [14]. Our survey of the β -C–H agostic structure of the *i*-Pr system reveals a very similar functional dependence. We have been unable to locate a BCP between the agostic hydrogen and the niobium centre using the PBE1PBE functional, despite the patently ‘agostic’ optimised structure in Table 1. The TPSS functional [35] generates an almost identical structure, but in this case a bond path between Nb and the β -H does emerge (Fig. 7). The Nb...H BCP is, however, very close to the ring critical point, and it is therefore unsurprising that very small changes in geometry or indeed methodology can cause them to merge into a singularity. The apparently erratic behaviour of the molecular graph is inti-

mately connected to the dependence of the structure on functional described previously: the very fact that the UEG limit is critical for the modelling of the β -agostic structure immediately tells us that the electron density in the important region between the Nb and H atoms is highly homogeneous, and it is precisely these situations where the characterization of the curvature of ρ is most difficult. In marked contrast to the β -CH agostic case, a Nb...H bond path is *never* found for the α -C–H agostic structure, regardless of the functional, apparently eliminating the possibility of a direct interaction between the metal centre and the C–H bond in this case.

The frontier Kohn–Sham orbitals of the α -agostic structure shown in Fig. 8 illustrate the very important point that the HOMO has dominant Nb–C σ bonding character and is strongly polarized towards the carbon. This is perhaps unsurprising, given the energy mismatch between the alkyl lone pair and the d orbitals of an early transition metal ion such as Nb, but it suggests that stabilisation of the alkyl lone pair will be the strongest driving force for distortions away from an idealised structure. The C–H bonding orbital, in contrast, is buried deep in the occupied manifold, and bringing this orbital into contact with the metal will yield a relatively small energetic gain. In these systems, the most readily available sink for the electron density in the alkyl lone pair is the π^* orbital on the alkyne unit, and the HOMO shows a distinct canting of the Nb–C $_{\alpha}$ σ orbital towards the alkyne ligand. This in turn forces the C $_{\alpha}$ –H bond towards the metal, but it is important to emphasise that it is being pushed into this position, not pulled! Similar features are apparent in the β -C–H agostic structure, suggesting that delocalization of the alkyl lone pair is a common mechanism for both. In addition, direct overlap of the metal and β -CH orbitals, apparent in the LUMO, also contributes to the stability of the system, although

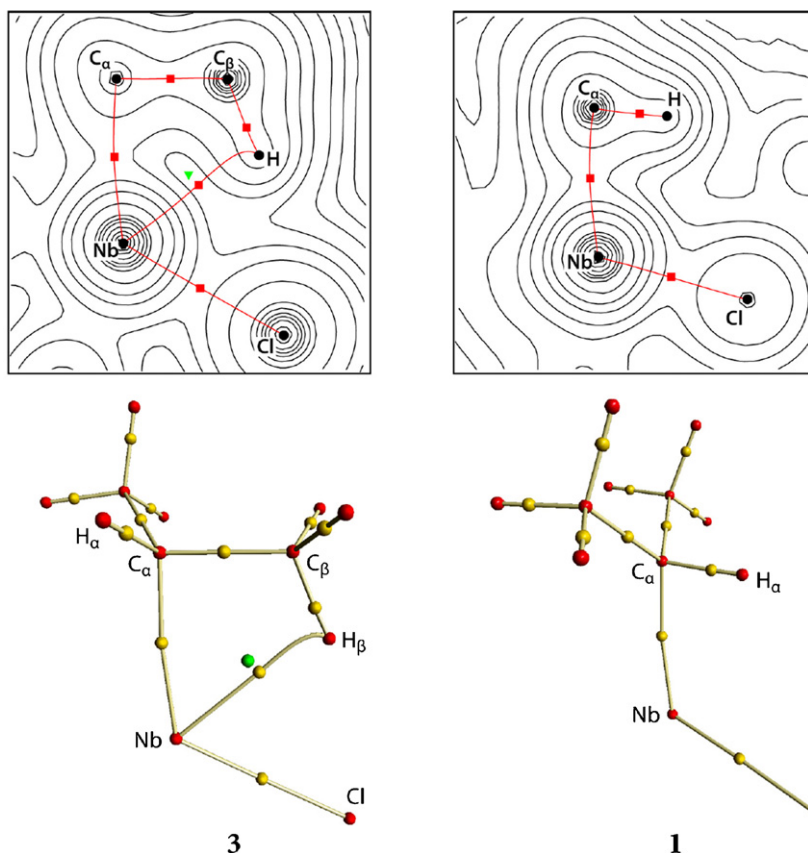


Fig. 7. Density maps (TPSS functional) drawn on the agostic planes (top) and partial molecular graphs (bottom) of isopropyl rotamers **3** and **1**: red spheres indicate nuclear attractors, yellow and green spheres correspond to (3, -1) bond and (3, +1) ring critical points, respectively.

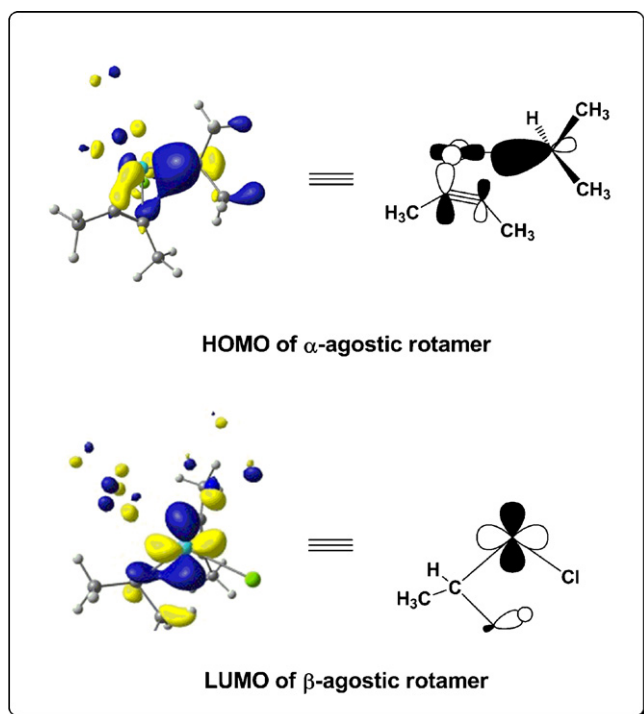


Fig. 8. Frontier Kohn-Sham orbitals of α - and β -C–H agostic structures of $\text{Tp}^{\text{Me}_2}\text{NbCl}(\text{MeC}\equiv\text{CMe})(i\text{-Pr})$. Contour value $0.0622 (\text{e}\text{\AA}^{-3})^{1/2}$.

the behaviour of the molecular graphs suggests that it is not the dominant mechanism. A natural bond orbital (NBO) [36] analysis confirms the qualitative interpretation of the Kohn–Sham orbitals: donor–acceptor interactions between the alkyl lone pair and the π^* orbitals of the alkyne ligand are similar in magnitude to direct interactions between the C–H bonding orbital and the metal centre in the β -agostic structure, and outweigh them in the α -agostic analogue.

This analysis places the emphasis firmly on stabilisation of the alkyl lone pair as the primary driving force for agostic distortions, striking resonance with earlier arguments put forward for early transition metal alkyls. Scherer et al. have argued that the key stabilising influence in these systems is the delocalisation of the M–C σ bonding electrons over the framework of the alkyl ligand itself – in effect negative hyperconjugation [14], while Eisenstein identified delocalisation of the lone pair into metal-based orbitals other than the one aligned along the M–C axis as the primary driving force [8]. Thus the need to stabilise the alkyl-based lone pair emerges as a common theme in early transition metal alkyls – the ligand will distort in such a way that the lone pair is directed towards the most accessible vacant orbital on the rest of the molecule, whether it be localised on the metal, on the alkyl ligand itself, or on other unsaturated ligands bound to the metal. This canting must necessarily force one of the substituents, X, on the α -carbon towards the metal centre, and hence cause strong distortions as measured by the M–C α –X angles. The reason why this canting forces one substituent into the ‘agostic position’, precisely as the traditional orbital description of agostic interactions would predict, (Fig. 1) is not yet fully understood, although it may be associated with a secondary role for this orbital interaction.

5. Concluding remarks

Niobium((tris)pyrazolyl)(chloride)(alkyne)(alkyl) complexes exhibit a rich structural chemistry in relation to the agostic inter-

actions between the alkyl group and the metal centre. Primary alkyl groups favour a relatively unusual α C–H agostic interaction over the more common β C–H agostic interaction, while secondary alkyl groups exhibit dynamic equilibria between α and β C–H agostic isomers, the former being dominant for cyclic alkyls but the latter for their acyclic analogues. The cyclopropyl complex presents a highly unusual case where an α C–C agostic interaction is favoured over α - or β -CH agostic alternatives. Hybrid DFT/MM calculations have allowed us to clarify the origins of this seemingly chaotic behaviour. There are in all cases three possible rotamers, corresponding to the 120° rotation around the Nb–C_{alkyl} bond, some or all of which may correspond to minima on the potential energy surface. Which of these is more stable depends on a subtle interplay of steric and electronic factors. For the CH agostic systems, the dominant structural control is a steric one, exerted by the pendant methyl groups in the Tp^{Me_2} ligand which force the bulkiest substituent on the α carbon away from the metal centre, between two of the methyl groups. The stereochemistry about the α carbon then completely determines which of the other two substituents lies in the agostic position, bisecting the C α –Nb–Cl angle. In cases where the α carbon carries two substituents of equal (or almost equal) bulk, as in the *i*-Pr or *sec*-Bu complexes, an equilibrium between different isomers emerges. In such circumstances, the relative stabilities of the α - and β -agostic structures are largely controlled by the ability of the alkyl ligand to distort at the α carbon to accommodate the steric and electronic requirements of the β -CH agostic structure. The reduced flexibility of the cyclic alkyls therefore naturally favours the α -agostic structure.

While the DFT/MM calculations reproduce the majority of the experimental observables, and offer valuable insights into the relative stabilities of the isomers, they do not offer insight into the fundamental origin of the agostic interactions themselves. Calculations performed using a full DFT protocol reveal that the chosen correlation functional plays a key role for the β -agostic structure, with only those that conform to the uniform electron gas limit successfully reproducing the experimental structure. The α -agostic structure is, in contrast, much less sensitive to functional, suggesting a rather different origin for this type of interaction. Our analysis of the electronic structure suggests that direct interactions between the C–H bond and the metal are of secondary importance in the β -agostic structure, and are completely absent in the α -agostic counterparts. Instead, the primary driving force for agostic distortions in these early transition metal systems is the stabilisation of the Nb–C σ bonding electrons by delocalisation into the vacant π^* orbitals of the alkyne co-ligand. The de-emphasis of direct overlap of C–H σ and metal-based orbitals is consistent with recent work by other groups suggesting that delocalisation of the high-lying M–C σ bonding electrons is a common driving force in early transition metal agostics [15].

Acknowledgements

We thank all our talented co-workers whose name appear in the references to these studies. This research was supported by the CNRS, the ICIQ foundation, the Spanish MICINN under projects CTQ2005-09000-CO1-02/BQU and Consolider Ingenio 2010 CSD2006-0003, the Catalan DURSI under project 2005SGR00715 and the EPSRC under project EP/C534425/2.

References

- [1] M. Brookhart, M.L.H. Green, *J. Organomet. Chem.* 250 (1983) 395.
- [2] M. Brookhart, M.L.H. Green, L.-L. Wong, *Prog. Inorg. Chem.* 36 (1988) 1.
- [3] (a) S. Trofimenko, *J. Am. Chem. Soc.* 90 (1968) 4754;
(b) S. Trofimenko, *Inorg. Chem.* 9 (1970) 2493.
- [4] F.A. Cotton, T. LaCour, A.G. Stanislawski, *J. Am. Chem. Soc.* 96 (1974) 754.

- [5] (a) M.D. Butts, J.C. Bryan, X.-L. Luo, G.J. Kubas, *Inorg. Chem.* 36 (1997) 3341;
(b) G.I. Nikonov, P. Mountford, S.K. Ignatov, J.C. Green, M.A. Leech, G.L. Kuzmina, A.G. Razuvaev, N.H. Rees, A.J. Blake, J.A.K. Howard, D.A. Lemenovskii, *J. Chem. Soc. Dalton Trans.* (2001) 2903.
- [6] (a) T. Ziegler, V. Tschinke, A. Becke, *J. Am. Chem. Soc.* 109 (1987) 1351;
(b) Y. Han, L. Deng, T. Ziegler, *J. Am. Chem. Soc.* 119 (1997) 5939.
- [7] A. Demolliens, Y. Jean, O. Eisenstein, *Organometallics* 5 (1986) 1457.
- [8] O. Eisenstein, Y. Jean, *J. Am. Chem. Soc.* 107 (1985) 1177.
- [9] R.J. Goddard, R. Hoffmann, E.D. Jemmis, *J. Am. Chem. Soc.* 102 (1980) 7667.
- [10] F. Maseras, A. Lledós, E. Clot, O. Eisenstein, *Chem. Rev.* 100 (2000) 601.
- [11] (a) R.F.W. Bader, *Atoms in Molecules: A Quantum Theory*, Oxford University Press, Oxford, 1990;
(b) P. Popelier, *Atoms in Molecules: An Introduction*, Pearson Education, Harlow, 2000;
(c) R.F.W. Bader, *Chem. Rev.* 91 (1991) 893;
(d) P.L.A. Popelier, *Struct. Bond.* 115 (2005) 1.
- [12] (a) J. Cioslowski, S.T. Mixon, *J. Am. Chem. Soc.* 114 (1992) 4382;
(b) A. Haaland, D.J. Shorokhov, N.V. Tverdova, *Chem. Eur. J.* 10 (2004) 416;
(c) R.F.W. Bader, D.-C. Fang, *J. Chem. Theory Comput.* 1 (2005) 403;
(d) F. Matta, J. Hernandez-Trujillo, T.-H. Tang, R.F.W. Bader, *Chem. Eur. J.* 9 (2003) 1940;
(e) J. Poater, M. Sola, F.M. Bickelhaupt, *Chem. Eur. J.* 12 (2006) 2889;
(f) R.F.W. Bader, *Chem. Eur. J.* 12 (2006) 2896;
(g) J. Poater, M. Sola, F.M. Bickelhaupt, *Chem. Eur. J.* 12 (2006) 2902.
- [13] P.L.A. Popelier, G. Logothetis, *J. Organomet. Chem.* 555 (1998) 101.
- [14] (a) W. Scherer, G.S. McGrady, *Angew. Chem. Int. Ed.* 43 (2004) 1782;
(b) W. Scherer, P. Sirsch, D. Shorokhov, M. Tafipolsky, G.S. McGrady, E. Gullo, *Chem. Eur. J.* 9 (2003) 6057.
- [15] (a) A. Haaland, W. Scherer, K. Ruud, G.S. McGrady, A.J. Downs, O. Swang, *J. Am. Chem. Soc.* 120 (1998) 3762;
(b) W. Scherer, W. Hieringer, M. Spiegler, P. Sirsch, G.S. McGrady, A.J. Downs, A. Haaland, B. Pedersen, *Chem. Commun.* (1998) 2471;
(c) W. Scherer, P. Sirsch, M. Grosche, M. Spiegler, M. Mason, M.G. Gardiner, *Chem. Commun.* (2001) 2072.
- [16] T.S. Thakur, G.R. Desiraju, *J. Mol. Struct. Theochem.* 810 (2007) 143.
- [17] I. Vidal, S. Melchor, I. Alkorta, J. Elguero, M.R. Sundberg, J.A. Dobado, *Organometallics* 25 (2006) 5638.
- [18] E. Clot, O. Eisenstein, *Struct. Bond.* 113 (2004) 1.
- [19] (a) M. Etienne, R. Mathieu, B. Donnadiou, *J. Am. Chem. Soc.* 119 (1997) 3218;
(b) M. Etienne, *Organometallics* 13 (1994) 410.
- [20] J. Jaffart, R. Mathieu, M. Etienne, J.E. McGrady, O. Eisenstein, F. Maseras, *J. Chem. Soc. Chem. Commun.* (1998) 2011.
- [21] J. Jaffart, M. Etienne, F. Maseras, J.E. McGrady, O. Eisenstein, *J. Am. Chem. Soc.* 123 (2001) 6000.
- [22] J. Jaffart, M. Etienne, M. Reinhold, J.E. McGrady, F. Maseras, *Chem. Commun.* (2003) 876.
- [23] J. Jaffart, M.L. Cole, M. Etienne, M. Reinhold, J.E. McGrady, F. Maseras, *Dalton Trans.* (2003) 4057.
- [24] M. Besora, F. Maseras, J.E. McGrady, P. Oulié, D.H. Dinh, C. Duhayon, M. Etienne, *Dalton Trans.* (2006) 2362.
- [25] J. Jaffart, C. Nayral, R. Choukroun, R. Mathieu, M. Etienne, *Eur. J. Inorg. Chem.* (1998) 425.
- [26] M.D. Fryzuk, S.A. Johnson, S.J. Rettig, *J. Am. Chem. Soc.* 123 (2001) 1602.
- [27] F. Maseras, *Chem. Commun.* (2000) 1821.
- [28] G. Ujaque, F. Maseras, *Struct. Bond.* 112 (2004) 117.
- [29] L. Cucurull-Sanchez, F. Maseras, A. Lledós, *Inorg. Chem. Commun.* 11 (2000) 590.
- [30] F. Maseras, K. Morokuma, *J. Comput. Chem.* 16 (1995) 1170.
- [31] S. Dapprich, I. Komaromi, K.S. Byun, K. Morokuma, M.J. Frisch, *J. Mol. Struct. (Theochem.)* 461 (1999) 1.
- [32] D.A. Pantazis, J.E. McGrady, F. Maseras, M. Etienne, *J. Chem. Theory Comput.* 3 (2007) 1329.
- [33] R. Colle, D. Salvetti, *Theor. Chim. Acta* 37 (1975) 329.
- [34] D.A. Pantazis, J.E. McGrady, M. Besora, F. Maseras, M. Etienne, *Organometallics* 27 (2008) 1128.
- [35] J. Tao, J.P. Perdew, V.N. Staroverov, G.E. Scuseria, *Phys. Rev. Lett.* 91 (2003) 146401.
- [36] A.E. Reed, L.A. Curtiss, F. Weinhold, *Chem. Rev.* 88 (1988) 899.